

Cite this: *Soft Matter*, 2019,  
15, 8578

## Reversible temperature-controlled gelation in mixtures of pNIPAM microgels and non-ionic polymer surfactant†

S. L. Fussell, \*abc K. Bayliss,<sup>a</sup> C. Coops,<sup>a</sup> L. Matthews, ac W. Li, d W. H. Briscoe, <sup>a</sup> M. A. Faers,<sup>e</sup> C. P. Royall abc and J. S. van Duijneveldt <sup>a</sup>

We investigate the reversible gelation of poly(*N*-isopropylacrylamide) (pNIPAM) microgels in the presence of triblock-copolymer (PEO–PPO–PEO type) surfactant. We demonstrate that the association of these polymers with the microgel particles at elevated temperature is responsible for the gelation, due to the temperature responsive nature of the components. This is highlighted by an increase in the apparent hydrodynamic diameter of the particles in dynamic light scattering experiments, which only occurs above the volume phase transition temperature of pNIPAM. The gels that result shrink over a time period much larger than that of the collapse of pNIPAM microgels, and retain the shape of the container they form in. We investigate the mechanism that leads to this gelation and the structure of the gels that result. Confocal microscopy experiments show that both polymers are present in the gel network, indicating that an associative mechanism is responsible for the gelation. We vary the pNIPAM particle architecture to further investigate the gelation process, and find that the cross-link distribution plays a key role in the gelation mechanism, where for uniformly cross-linked particles the gelation is not observed. This shows that the fuzzy corona of the pNIPAM microgels is involved in the association of the polymers, allowing the triblock-copolymer to penetrate the outer corona of the microgels and bridge the particles. The phase transition observed is close to physiological conditions, so these gels have the potential for use in biomedical applications, including tissue engineering.

Received 28th June 2019,  
Accepted 11th October 2019

DOI: 10.1039/c9sm01299k

rsc.li/soft-matter-journal

## 1 Introduction

Microgels are soft cross-linked polymer particles that form stable colloidal suspensions.<sup>1</sup> Due to their polymeric composition, microgels are responsive to external stimuli including light,<sup>2</sup> pH<sup>3</sup> and temperature,<sup>4</sup> with the result being a change in the particle size.<sup>5</sup> Poly(*N*-isopropylacrylamide) (pNIPAM) is a temperature responsive polymer which can be synthesised to form microgels. pNIPAM has a volume phase transition temperature ( $T_{VPT}$ ) at 32 °C<sup>6</sup> where the particles collapse and expel water from the interior.<sup>7</sup> This  $T_{VPT}$  is constant for pure pNIPAM

systems, irrespective of concentration, molecular weight<sup>8</sup> or architecture,<sup>9</sup> but can be altered by the presence of additives such as salt<sup>10</sup> and surfactant.<sup>11</sup> Microgels, whilst in their swollen state, consist of polymer chains in a random coil like conformation, with the structure being constrained by the cross-linked polymer.<sup>12</sup> When the deswollen state is favoured, the chains collapse and a smaller volume is taken up by the more compressed conformation.<sup>13</sup> The behaviour of microgel systems can be described using equilibrium swelling theory, where the swelling of cross-linked polymer particles can be characterised using the cross-link density of the system and the quality of the solvent.<sup>14</sup> pNIPAM is often the focus of biomedical research, due to its  $T_{VPT}$  being close to physiological conditions.<sup>15</sup> pNIPAM microgels are often considered for triggered drug delivery systems,<sup>16</sup> whereas pNIPAM hydrogels are considered as a material for tissue engineering.<sup>17</sup>

Although microgels can be thought of as particles, it is synthetically challenging to make microgels with a uniform distribution of cross-links and bound charge.<sup>18</sup> Microgels are very stable to aggregation, due to the particles often having associated charge at their surface, as a result of the initiator used, and the fuzzy corona that forms from the linear polymer

<sup>a</sup> School of Chemistry, University of Bristol, Cantock's Close, Bristol, BS8 1TS, UK  
E-mail: Sian.fussell@bristol.ac.uk

<sup>b</sup> HH Wills Physics Laboratory, University of Bristol, Tyndall Avenue, Bristol, BS8 1TL, UK

<sup>c</sup> Bristol Centre for Functional Nanomaterials, University of Bristol, Tyndall Avenue, Bristol, BS8 1TL, UK

<sup>d</sup> School of Chemistry, Capital Normal University, No. 105 Xisanhuan Road, Haidian District, Beijing, 100048, China

<sup>e</sup> Bayer AG, Alfred Nobel Str. 50, 40789 Monheim, Germany

† Electronic supplementary information (ESI) available. See DOI: 10.1039/c9sm01299k

chains that dangle from the densely cross-linked core.<sup>19,20</sup> This fuzzy corona is known to affect the interactions between microgel particles, and make them more stable to aggregation.<sup>21</sup> There have been few studies describing the surface properties of the pNIPAM microgels, and for most systems the length and density of the extending polymer layer is unknown.<sup>22</sup> pNIPAM is known to spontaneously form cross-linked particles even without addition of a cross-linking agent during synthesis,<sup>23</sup> however, the addition of cross-linker allows the control of swelling capacity of the particles.<sup>24</sup>

There are several common mechanisms that result in the formation of colloidal gels.<sup>25</sup> Often the mechanism of spinodal decomposition is found,<sup>26</sup> where spontaneous demixing results in the formation of two phases, and an arrested gel network results from the rigid local arrangements of particles.<sup>27</sup> Polymers are also known to bridge colloidal particles to form percolating networks, where polyelectrolytes of opposite charge to the colloid can adhere to surface with extended polymer loops. These can attach to a bare patch on a neighbouring colloid, resulting in network formation.<sup>28–30</sup> Microgels have also been shown to induce colloidal gel formation, where both depletion and microgel bridging mechanisms are observed.<sup>31,32</sup>

Due to microgels having tunable softness,<sup>33</sup> they are increasingly being used as model colloidal systems,<sup>19</sup> and in addition to liquids and gels they can form colloidal crystals and glasses.<sup>34,35</sup> Microgels are unusual in this inherent particle softness and are often considered to behave inbetween a hard sphere and a polymer.<sup>36</sup> Microgels are of great interest in the field of stimuli responsive systems due to their properties being dependent on physical conditions, such as temperature, resulting in the ability to control gelation using external stimuli.<sup>37,38</sup>

Linear pNIPAM is known to form hydrogels upon heating and is often the focus for applications in the field of tissue engineering.<sup>39</sup> pNIPAM microgels are also capable of aggregation to form temperature responsive gels in the presence of salt, where the salt screens charges on the particle surface leading to attractive forces dominating and therefore, gelation.<sup>40</sup> These macrogels form reversibly on heating and were shown to undergo syneresis. All examples of pNIPAM microgels forming networks in the literature to our knowledge are a result of the charge screening effect of salt. It has also been observed in the literature that syneresis of pNIPAM gels can be suppressed with the addition of poly-ethyleneoxide (PEO), however this resulted in a decrease of the gel strength.<sup>41</sup>

The interaction of pNIPAM-*co*-acrylic acid microgels with non-ionic additives, such as PEO<sup>42</sup> and non-ionic surfactant<sup>43</sup> has been investigated in the literature. These non-ionic species were shown to interact with the microgels, through hydrogen bonding between the carboxyl groups on the acrylic acid and the hydrogen on the amide group of NIPAM, and were able to penetrate into the microgel periphery. The ease of penetration can be related to the degree of cross-linking and the ratio of pNIPAM: acrylic acid, where with increasing acrylic acid content and decreasing cross-link density increasing amounts of non-ionic species penetrate inside the microgels. It was also found that for microgels of a lower cross-link density that

micelles of non-ionic surfactant could form inside the pores. Bradley *et al.* furthermore showed that the non-ionic surfactant also absorbed to the linear analogue of pNIPAM.<sup>43</sup>

In this paper we demonstrate an alternative gelation mechanism for pNIPAM that uses the interaction with a triblock-copolymer surfactant to form reversible, temperature responsive macrogels of pNIPAM. The mechanism for gelation here is the high temperature association of these species, likely controlled by the increasing hydrophobicity of pNIPAM with increasing temperature. In this work we demonstrate the properties of this material and provide evidence for the temperature responsive association of these species. This gelation process is fully reversible where the solution transitions from colloidal suspension to gel at elevated temperatures. The system also forms a collapsing gel network that shrinks over time, at temperatures above the aggregation temperature.

## 2 Experimental

### 2.1 Materials

All chemicals were used as received without further purification. For the microgel synthesis *N,N'*-methylenebis(acrylamide) (99% Sigma Aldrich), *N*-isopropylacrylamide (99% Acros Organics), potassium persulfate (>99% Sigma Aldrich), sodium dodecylbenzenesulfonate (technical grade Sigma Aldrich), fluorescein isothiocyanate (98% Sigma Aldrich), allylamine (98% Sigma Aldrich), tetramethylene-ethyleneamide (98% Sigma Aldrich), ammonium persulfate (Life Sciences) and methacryloxyethyl thiocarbonyl rhodamine B (Polysciences) were used. Nile red (technical grade Sigma Aldrich) was used to label the triblock-copolymer surfactant. For deuterated pNIPAM samples d7-NIPAM (>98% Polymer Source Inc.) was used.

### 2.2 pNIPAM microgel synthesis

The general method used to make pNIPAM microgels was adapted from methods reported by McPhee *et al.*<sup>44</sup> The addition of anionic surfactants to the synthesis allows for control over the microgel size, and produces colloidally stable particles much smaller than accessible using the surfactant free method. In general, each synthesis was conducted under an inert atmosphere in a 1 l three necked round bottom flask, fitted with an overhead stirrer, a condenser and an argon inlet. All monomers, cross-linker and surfactant were added to the flask and heated to 70 °C, the initiator potassium persulfate was then added slowly to the reaction mixture and the reaction left to proceed for 4 hours stirring at a rate of 300 rpm. The microgels produced were then dialysed against deionised water for 2 weeks in order to remove unreacted monomer and surfactant. Typically 12.5 g of *N*-isopropylamide, 1.0 g of *N,N'*-methylenebis(acrylamide) and 0.5 g of sodium dodecylbenzenesulfonate were added to 475 ml of deionised water, then 0.5 g of potassium persulfate added as a 2 wt% solution. For the fluorescein labelled particles, 9 mg of fluorescein isothiocyanate and 15 µl 3-amino-propene were added to 38 ml of a solution of 10<sup>-4</sup> M sodium hydroxide, in order to synthesise a polymerisable fluorescein

dye molecule, this solution was then added to the reaction mixture with the monomers.<sup>45</sup>

### 2.3 Uniformly cross-linked pNIPAM microgel synthesis

Uniformly cross-linked particles were synthesised using the feeding method. Typically, the total amount of reagents used were 5.6 g of *N*-isopropylamide, 0.42 g of *N,N'*-methylenebis(acrylamide) and 0.056 g of sodium dodecylbenzenesulfonate. 280 ml of water was heated to 80 °C under an argon atmosphere.<sup>46</sup> Then 8% of the monomers were added to 18 ml of water, and 1 ml of sodium dodecylbenzenesulfonate was added as a 6 wt% solution. The initiator ammonium persulphate was then added to the solution as a 1 ml 6 wt% solution. The remaining 92% of the monomers were dissolved in 28 ml of water and fed into the reaction at a rate of 0.2 ml min<sup>-1</sup>, in order to obtain uniformly cross-linked particles. Once the monomer feeding was complete, the solution was rapidly cooled to prevent further polymerization. The resultant particles were then dialysed for 2 weeks against deionised water. Methacryloxyethyl thiocarbonyl rhodamine B was added to the synthesis as a co-monomer at 0.052% by weight of the NIPAM monomer.

### 2.4 Linear pNIPAM synthesis

The synthesis of linear pNIPAM was adapted from the method reported by Gao *et al.*<sup>47</sup> 7.55 g NIPAM and 0.0083 g potassium persulfate were added to 100 ml of water in a 200 ml Schott bottle. This solution was purged with argon for 20 minutes. 0.3 ml of tetramethyleneethylenamide was then added and the reaction mixture immersed into an ice bath for 12 hours. The resultant polymer solution showed a large increase in viscosity, indicating that the polymerization had occurred. The polymer solution was then precipitated using a 50/50 by volume mixture of acetone/water and filtered. The precipitate was then dried in a oven at 50 °C and redispersed in deionised water for investigation.

### 2.5 Triblock-copolymer surfactant

The triblock-copolymer used as part of this work was supplied by Croda and is known commercially as Synperonic PE/P105, a summary of the triblock-copolymer surfactant's characteristic properties are included in Table 1. Over the concentration and temperature range studied, it is expected that the triblock-copolymer phase is individual spherical micelles.<sup>48</sup>

**Table 1** Table summarising characteristic properties of the triblock-copolymer micelles of Synperonic PE/105. Poly-ethyleneoxide (PEO), poly-propyleneoxide (PPO), critical micelle concentration (CMC),<sup>48,49</sup> critical micellisation temperature (CMT)<sup>48,49</sup>

Property	Literature value
Mol. wt	6500 g mol <sup>-1</sup>
No. PEO units	74
No. PPO units	56
CMC (25 °C)	0.3 wt%
CMC (35 °C)	0.005 wt%
CMT	0.25 wt% (25 °C)

### 2.6 Particle characterisation

All dynamic light scattering (DLS) measurements were taken using a Malvern Autosizer 4800 with a 532 nm laser at a 90° scattering angle. Samples were allowed to equilibrate for 15 minutes at each temperature. All samples were diluted with deionised water to the desired concentration.

### 2.7 Characterisation of phase behaviour

The temperature dependent phase behaviour of the system was investigated using 0.5 g mixtures of pNIPAM microgels and triblock-copolymer placed in 1.75 ml sealed vials. The sample vials were then submerged into boiling water and the phase behaviour recorded.

### 2.8 Microscopy

For confocal microscopy, all images were taken using a Leica (SP-8) confocal microscope. For samples labelled with Nile red, a 543 nm HeNe laser was used to excite the dye. For samples labelled with fluorescein, a 488 nm Argon laser was used to excite the dye. All images were taken using a Bioscience Tools objective heater with a TC-1-100s temperature controller set to 50 °C and a Linkam PE120 heating stage set also to 50 °C. For the sample preparation, a drop of solution was added to the centre of a Avery Reinforcement Rings White sticker (Office Depot) attached to a microscope slide, a cover slip was then placed above and the edges sealed with using UV-curing glue. This created a thin, confined sample cell of diameter 5 mm and a thickness of 200 µm.

In order to label the triblock-copolymer surfactant, Nile red was used. 1 M solutions of Nile red were dissolved in methanol. Then this was added to triblock-copolymer solution at a concentration of 1 mM Nile red per 0.6 g of triblock-copolymer. Once the Nile red was added to the triblock-copolymer solution the samples were left on a roller plate to equilibrate overnight.

All differential interference contrast microscopy images were taken using an Olympus BX-51 DIC microscope, using a 20× objective and a Pixelink 5MP colour CCD PL-B625CU camera. The temperature of the slide was controlled using a Linkam PE120 heating stage. For the sample preparation, the method was the same as described for confocal microscopy, except the edges were sealed with nail varnish.

### 2.9 Small angle neutron scattering

The small angle neutron scattering (SANS) data was collected using the SANS2D beam line at the ISIS pulsed neutron source. All samples were run in a 2 mm quartz Hellma cell. Samples were prepared using H-Synperonic PE/P 105 and d-pNIPAM microgels. NMR revealed that the d-NIPAM monomer was d5-NIPAM (where 5 of the hydrogens in the structure have been replaced by deuterium), estimated using peak integration to determine the number of hydrogens in the sample (Fig. S1, ESI†). This was used to estimate the scattering length density (SLD) of the microgels, in order to contrast match with a H<sub>2</sub>O/D<sub>2</sub>O mixture, the solvent used was 0.35 : 0.65 mass ratio H<sub>2</sub>O/D<sub>2</sub>O. The SLDs are included in Table 2. Samples were run at 25 °C and 40 °C. Samples were counted for 20 µA h.

**Table 2** Calculated SLDs used for SANS fitting

Chemical	Calculated SLD ( $10^{-6} \text{ Å}^{-2}$ )
d5-NIPAM	3.78
H-Syneronic PE/P105	0.49
$\text{H}_2\text{O}/\text{D}_2\text{O}$ solvent mixture	3.78

The d-NIPAM microgels were synthesised using methods outlined in Section 2.4. The concentration and scale of the synthesis was reduced, 0.09 g of d5-NIPAM, 0.0109 g of *N,N'*-methylenebis(acrylamide) and 0.01 g of sodium dodecyl sulfate we dissolved in 10 ml of MilliQ water. 0.006 g of ammonium persulphate was added as a 2 wt% solution.

For all samples the scattering from the empty cell and the  $\text{H}_2\text{O}/\text{D}_2\text{O}$  solvent mixture were subtracted from the raw data. For the fitting, the triblock-copolymer surfactant SANS data was fitted using the polymer micelle model.<sup>50</sup> A Guinier fit (Fig. S9, ESI†) was used to estimate the radius of gyration from the low  $Q$  signal for the high temperature mixtures of pNIPAM and triblock-copolymer surfactant.

### 3 Results and discussion

All particles used in this work were synthesised using precipitation polymerisation, with added surfactant to control the particle size unless otherwise stated. The particles were then characterised using dynamic light scattering (DLS), to obtain the hydrodynamic diameter of the particles and to study the deswelling behaviour (Fig. S2, ESI†). For all the results included, the diameter of the swollen particles was approximately 100 nm unless otherwise stated. A summary of the pNIPAM particles used in this work is included in Table 3.

In this work we present evidence for the temperature responsive association of pNIPAM microgel particles and triblock-copolymer surfactant. We use DLS to investigate the associative behaviour at low particle concentrations, to highlight the interaction of the polymer with individual microgels. SANS was used to look at the structure of the triblock-copolymer micelles in mixtures with pNIPAM at elevated temperatures. We use microscopy techniques to investigate the composition of the gel, where selective labelling using fluorophores allows each component of the gel to be independently excited using confocal microscopy. We also utilize the tuneable synthesis of pNIPAM microgels to understand the molecular interaction of these particles with the triblock-copolymer micelles.

**Table 3** Summary of the pNIPAM particles used throughout this paper. The sample prepared using the feeding method produce uniformly cross-linked (UCL) particles.  $d_{40}/d_{25}$  is the deswelling ratio of pNIPAM microgels, comparing the hydrodynamic diameters at 40 °C and 25 °C

Particle	Particle diameter (nm)	Synthetic method	Deswelling ratio $d_{40}/d_{25}$	Figure particle referenced
Unlabelled pNIPAM 1	$107.3 \pm 0.5$	Precipitation	0.54	Fig. 2 and 3
Unlabelled pNIPAM 2	$98.6 \pm 1.0$	Precipitation	0.58	Fig. 4 and 7
Fluorescein labeled	$145.6 \pm 0.3$	Precipitation	0.55	Fig. 1
Rhodamine B labeled	$260.0 \pm 2.6$	Feeding	0.47	Fig. 6
Deuterated pNIPAM	$101.3 \pm 10.2$	Precipitation	0.55	Fig. 5

### 3.1 Evidence of association

Evidence of the association of these temperature sensitive polymers was obtained using confocal microscopy. This high resolution imaging technique is capable of differentiating species in the gel network. The pNIPAM and the triblock-copolymer are each labeled using dyes with a different excitation/emission wavelength. The images (Fig. 1) show that the triblock-copolymer is present in the gel network, where the signals from both species overlap. The pNIPAM microgels are labelled with fluorescein monomer, added as a co-monomer during the synthesis of pNIPAM microgels described in Section 2.2. The triblock-copolymer is labelled using the favourable adsorption of hydrophobic Nile red inside the polymeric surfactant micelles. Nile red is a solvatochromic dye, where the excitation is dependent on the environment the dye resides in. We found that the emission of the dye in the presence of pNIPAM and the triblock-copolymer was equivalent to the emission observed for the triblock-copolymer alone, observed using fluorescence spectroscopy (Fig. S3, ESI†). Fig. 1 contains typical confocal images of the gels observed for this system. The green image (Fig. 1a) shows the fluorescent signal from pNIPAM, the red image (Fig. 1b) shows the signal from the triblock-copolymer and the yellow signal (Fig. 1c) indicates the fluorescent signal where both fluorophores are present. This is strong evidence that the association of these species results in the gelation, rather than depletion, as the images show the fluorescent signal from the labelled triblock-copolymer coming from the same region as the microgels. For depletion it would be expected that the fluorescent signal for the triblock-copolymer would predominantly be found in the areas where the solvent is present. The gels that result from pNIPAM and triblock-copolymer are also stable to dilution; if an excess of water is added to a gel sample at elevated temperatures, diluting the sample to a concentration that would not form gels, the gel persists for time periods longer than expected for dissolution. This again suggests that depletion is not the mechanism

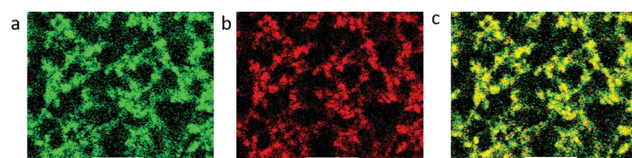
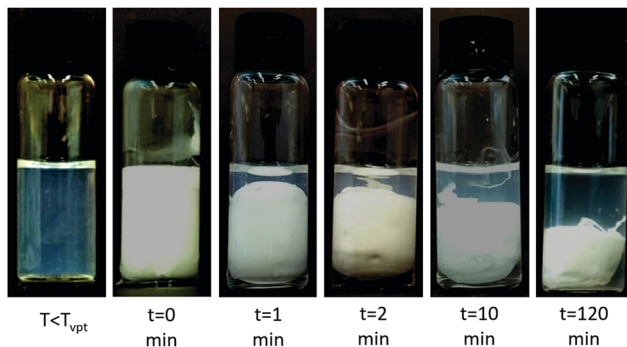


Fig. 1 Confocal microscopy images of 3 wt% pNIPAM and 3 wt% triblock-copolymer, fluorescence from fluorescein labelled microgels (a), fluorescence from Nile red labelled triblock-copolymer (b) and fluorescence from both components (c). All images are taken at 50 °C, scale bar 10 μm.

responsible for gelation. Confocal microscopy is not capable of imaging the individual particles and micelles in solution as this is beyond the resolution of the technique, so details of how the triblock-copolymer associates with the pNIPAM at the individual molecule level cannot be obtained using this technique.

### 3.2 Macroscopic gel behaviour

As part of this investigation it was observed that when concentrated samples of pNIPAM microgels and a triblock-copolymer were heated, the systems form macroscopic gels. These gels are originally space spanning, then undergo syneresis when left at



**Fig. 2** Gelation of pNIPAM microgels in the presence of triblock-copolymer at elevated temperature. The images are of the same sample held at temperatures above the  $T_{VPT}$  for an extended amount of time, highlighting the syneresis effect. These images are taken in a 3.5 ml vial, and the particles in these images are 107 nm in diameter when swollen. Concentration is 4 wt% pNIPAM, 4 wt% triblock-copolymer.

elevated temperatures. Hereby, the gels contract away from the container edges, holding the shape of the container and leaving a liquid supernatant. This supernatant was shown to contain solely triblock-copolymer, where the hydrodynamic diameter measured on the DLS was equivalent to pure triblock-copolymer solution. An example of how the gel collapses/coarsens over time is included in Fig. 2. This gelation is fully reversible and can be repeated upon temperature cycling.

A summary of the phase behaviour of the system is included in Fig. 3. The observed trend is that at low pNIPAM concentrations (1 wt%), microscopic aggregates form, indicated by an increase in the opacity of the sample, much larger than for pNIPAM alone. With increasing pNIPAM concentration ( $> 2$  wt%) an incomplete gel network forms, where a solid gel can be seen to form, but the surrounding supernatant remains opaque like pure pNIPAM samples. DLS indicates that there are pNIPAM microgels present in the supernatant, showing that some pNIPAM remains free and is not incorporated into the network (Fig. S4, ESI†). At the high pNIPAM concentrations ( $> 3$  wt%) complete collapsing gel networks result. The supernatant was shown to contain only the triblock-copolymer, again evidenced using DLS, where the diameter of the aggregates present in the supernatant were similar to that of triblock-copolymer micelles (Fig. S4, ESI†). The concentration of triblock-copolymer required to form gels decreases with increasing pNIPAM concentration. As the concentration of particles increases so does the ability of the particles to aggregate, hence the decreasing concentration of surfactant necessary for percolating networks to form. The triblock-copolymer is always in excess in the system where gels form, and found to be present in the supernatant,

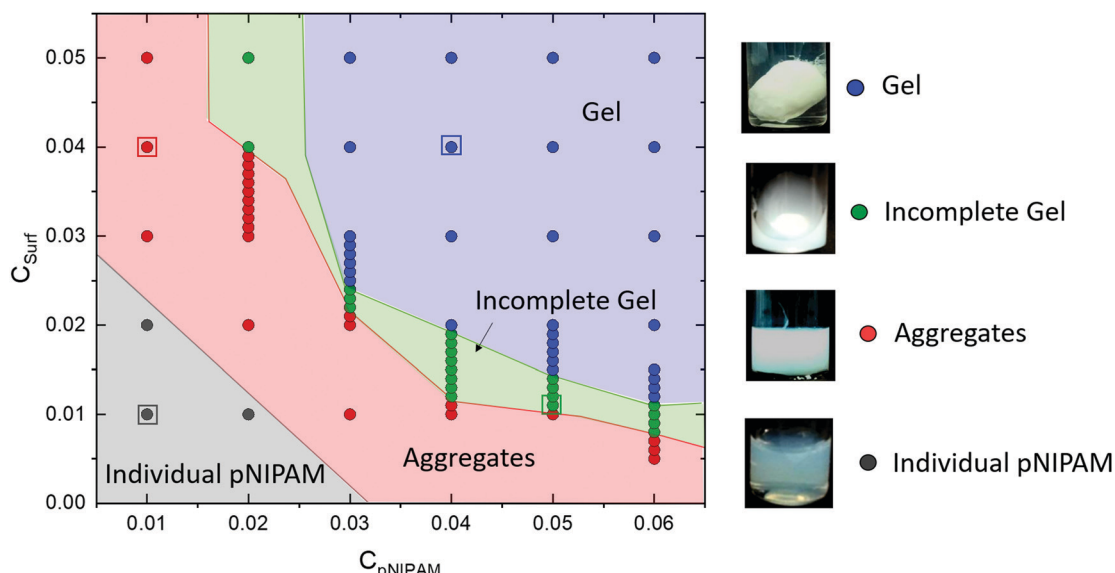


**Fig. 3** Phase diagram for mixtures of pNIPAM and triblock-copolymer surfactant. All of the data was collected after samples were held above the  $T_{VPT}$  for several minutes to allow syneresis to occur, by submerging the sample into freshly boiled water (Section 2.7). Grey circles indicate where no obvious aggregation could be observed, red circles represent liquid samples with macroscopic aggregates, green circles represent gels without all of the pNIPAM incorporated in the network, blue circles represent gels with all the pNIPAM incorporated into the network. Coloured regions of the phase diagram are to guide the eye. Photographs highlighted by a square illustrate the four types of behaviour of the sample. All concentrations are expressed as weight fractions.

hence the concentration of pNIPAM microgels in the system is the determining factor as to whether gelation occurs.

### 3.3 Low concentration behaviour

**3.3.1 Dynamic light scattering.** In order to gain an understanding of the low concentration interaction of pNIPAM and the triblock-copolymer, samples were studied using DLS. The results of this study have been included in Fig. 4. For all samples, the concentration of pNIPAM was set to 0.30 wt%, as the concentration needs to be sufficiently low in order to obtain accurate DLS results.

At temperatures below the  $T_{VPT}$  of pNIPAM, there is an initial decrease to the hydrodynamic diameter with heating, as seen for the pure pNIPAM. This shows that no interaction is observed between pNIPAM and the triblock-copolymer below the  $T_{VPT}$ . However, at temperatures higher than the  $T_{VPT}$ , there is a sharp increase in the hydrodynamic diameter, this is

shown in Fig. 4a. This shows that the association of the polymers is temperature responsive. The same effect is observed for all concentrations, however, as the concentration of triblock-copolymer increased this effect is heightened, this is summarized in Fig. 4b. This is due to the increased free triblock-copolymer concentration to decorate/penetrate the outer layer of the particles. The temperature at which this increase in hydrodynamic diameter occurs is the same for all concentrations of triblock-copolymer, within the temperature step range studied, indicating at these concentrations, the temperature response is dependent on the pNIPAM collapse.

A collapsed pNIPAM microgel is approximately 60 nm in diameter and the triblock-copolymer is approximately 20 nm in diameter, which would result in objects of approximately 100 nm being observed if the pNIPAM particles were completely collapsed and coated with triblock-copolymer. The particles are likely prevented from fully deswelling due to the triblock-copolymer

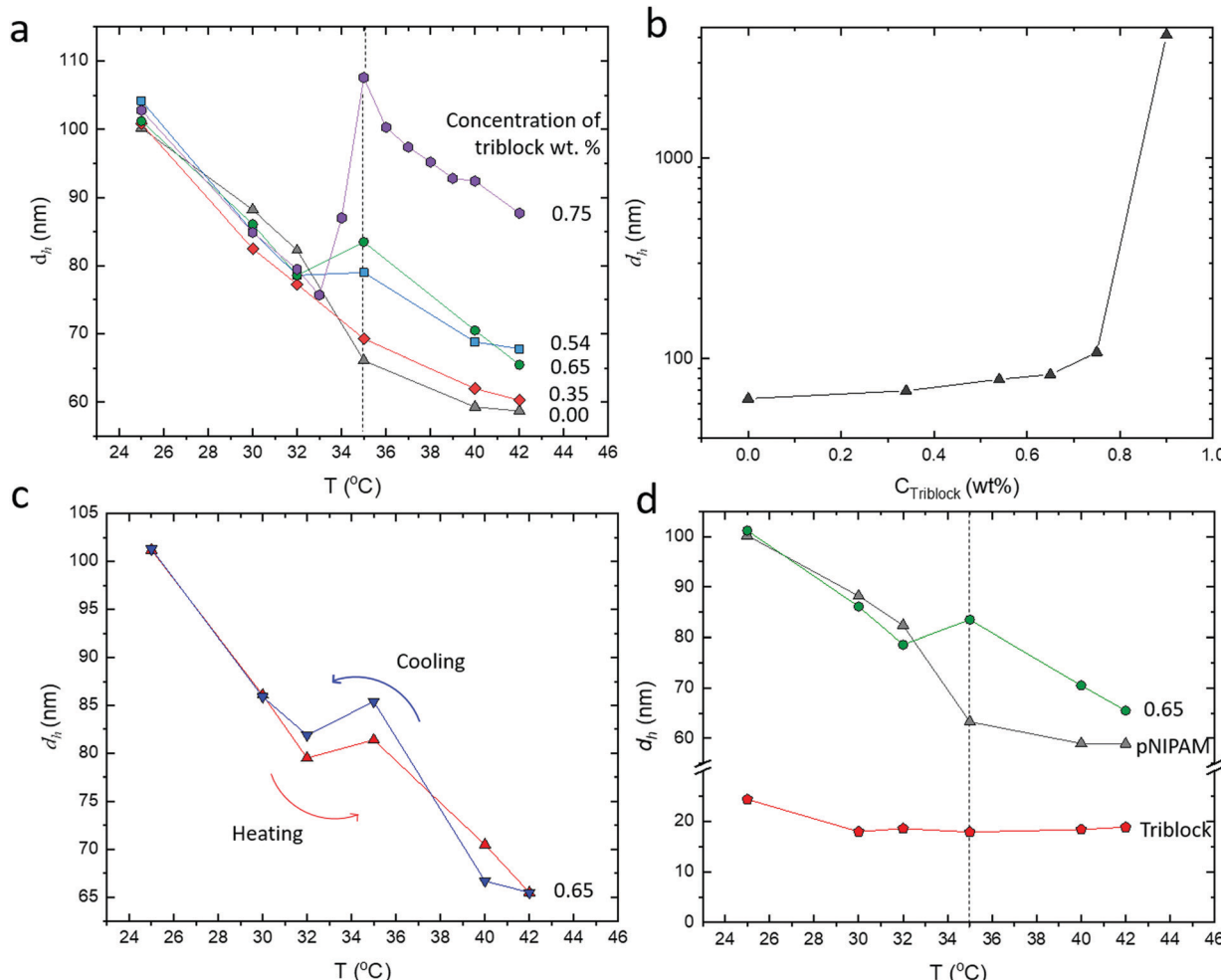


**Fig. 4** Dynamic light scattering results for mixtures of pNIPAM and triblock-copolymer. The concentration of pNIPAM is 0.3 wt% in all samples. (a) Effect of triblock-copolymer concentration on the hydrodynamic diameter of pNIPAM, as a function of concentration and temperature. (b) Effect of triblock-copolymer concentration on the hydrodynamic diameter at 35 °C. At concentrations higher than 0.75 wt% triblock-copolymer the samples start to aggregate, evidenced by a large increase in the observed hydrodynamic diameter. (c) Effect of heating and cooling the mixtures, 0.65 wt% triblock-copolymer is used. (d) Temperature dependent diameter of triblock-copolymer, concentration 2.5 wt%. The dashed black line indicates the temperature at which an increase in hydrodynamic diameter is observed for pNIPAM in the presence of triblock-copolymer. Data for 0.65 wt% triblock-copolymer and pure pNIPAM are included for comparison.

adsorbing into the pores of the microgel, which would result in the size of the objects observed in DLS being slightly larger than a collapsed microgel coated with triblock-copolymer micelles, this is observed for the 0.75 wt% sample (Fig. 4a, purple curve). If penetration inside the pores of the microgel was the only interaction between pNIPAM and triblock-copolymer surfactant, a similar DLS trend would be expected. The particles being prevented from deswelling would result in the increased instability of the particles and lead to gelation. This is due to the larger, denser microgels experiencing stronger van der Waals interactions. The phase diagram (Fig. 3) indicates that a decreasing amount of triblock-copolymer is needed to form gels with increasing pNIPAM concentration, the opposite effect expected for the latter destabilisation mechanism. Also the formation of incomplete gel networks would not be present, as all of the pNIPAM particles would be equally destabilised by the decreased deswelling. This indicates that a combination of penetration and decoration of the particles by the triblock-copolymer, and this resulting in polymer bridging, is the most likely mechanism for gelation.

The effect of cooling the sample was also studied using DLS, to confirm the peak in hydrodynamic diameter at 35 °C is not an artefact of the system initially aggregating, then rearranging to its equilibrium state after being held above the  $T_{VPT}$ . The peak in hydrodynamic diameter is observed for both the heating and cooling curves, showing that this is a temperature dependent effect and not due to the system being out of equilibrium, these DLS curves are shown in Fig. 4c. This result indicates that the microgel particles continue to deswell after association has occurred.

To highlight that the interaction is due to the collapse of the pNIPAM particles at the  $T_{VPT}$ , the temperature dependent diameter of the triblock-copolymer was measured, the results are included in Fig. 4d. The only observable difference was a slight decrease in the hydrodynamic diameter of the triblock-copolymer between 25 and 30 °C. This indicates that the temperature response of the triblock-copolymer at these concentrations is not responsible for the gelation, as there is little observable change in the triblock-copolymer's phase/aggregation behaviour.

As the temperature increases, the pNIPAM has a decreasingly favourable interaction with the surrounding solvent, which would explain the association, if the pNIPAM: polymer interaction becomes more favourable with temperature as the pNIPAM becomes increasingly hydrophobic. There are examples of polymers and micelles causing microgel swelling due to absorption into the particle.<sup>42</sup> The adsorption of PEO into pNIPAM-*co*-acrylic acid has been investigated, and that study does not suggest a temperature responsive adsorption but does show a decreased deswelling with temperature. The molecular weight of PEO used suggests that the mechanism of penetration into the periphery of the microgel is possible for the triblock-copolymer used as part of this study, as the molecular weight is sufficiently low.<sup>43</sup> The explanation for the association of PEO and pNIPAM was through hydrogen bonding with the amide group of the pNIPAM. If this is the mechanism of association for triblock-copolymer, this explains why the association is temperature

responsive, as pNIPAM decreasingly forms hydrogen bonds with water at elevated temperatures.<sup>9</sup> The phase behaviour of PEO and pNIPAM microgels was also investigated as part of this study (Fig. S5, ESI†). The results indicated that in the presence of PEO, pNIPAM microgels also aggregate, but resultant gels require higher concentrations than with the triblock-copolymer. Also, complete gels where all the microgels are present in the network were not observed for the PEO samples. The poly-propyleneoxide (PPO) block is what drives the polymer micelles to form, due to PPO being insoluble in water. This aggregation results in a dense PEO layer to interact with the NIPAM, hence the increased ability of the PEO block to form gels compared with the linear polymer. This suggests that the PEO block on the triblock-copolymer is capable of bridging microgel particles, resulting in bridging through micelles being the likely mechanism for gelation.

There is further evidence for the temperature responsive association when looking at the polydispersity (PDI) of the samples measured on the DLS. It is observed that there is an increase in PDI for the mixtures of pNIPAM and triblock-copolymer at low temperatures, expected due to the presence of 20 nm triblock-copolymer micelles. However, when the samples are heated above the  $T_{VPT}$  there is a sharp decrease in the PDI, due to fewer free surfactant micelles being present in the solution, due to the association (Fig. S6, ESI†). This shows that the increase in hydrodynamic diameter observed is due to the association of the polymers into well defined objects, rather than pNIPAM aggregates forming.

**3.3.2 Small angle neutron scattering.** SANS measurements were also collected for the low concentration mixtures of triblock-copolymer and pNIPAM microgels. The pNIPAM microgels were contrast matched with the solvent in order to only observe the scattering from solely the triblock-copolymer. The pure pNIPAM scattering is included in Fig. 5 (black curve), showing a very weak scattering highlighting that the scattering observed for the mixtures of pNIPAM microgels and triblock-copolymer is dominated by the triblock-copolymer surfactant. The deswelling of the d-pNIPAM microgels was measured using DLS (Fig. S8, ESI†). It revealed that the d-pNIPAM particles collapsed at a higher temperature than the equivalent hydrogenated particles, therefore the samples were run at 25 °C and 40 °C to ensure the microgels were above the  $T_{VPT}$  for the high temperature measurements.<sup>51</sup>

It can be observed that for all the samples there is a strong scattering signal from pure triblock-copolymer micelles (Fig. 5, blue and grey data). Details of the triblock-copolymer fits can be found in Table 4. The aggregation number was estimated from literature data.<sup>52</sup> The radius of gyration ( $R_g$ ) of the PEO polymer was estimated using the equation  $R_g = \sqrt{NLb/6}$ , where  $L$  is the contour length and  $b$  is the statistical segment length (the Kuhn length) of the chain. The literature values for PEO chains were used and are  $L = 2 \text{ \AA}$  and  $b = 10 \text{ \AA}$ .<sup>53</sup> The size of the triblock-copolymer micelles measured at 25 °C and 40 °C are comparable to the DLS data. There is evidence from the low temperature SANS that there are some impurities present in the 25 °C triblock-copolymer sample, which could indicate why the DLS data at 25 °C gives a larger hydrodynamic diameter than the higher temperatures.

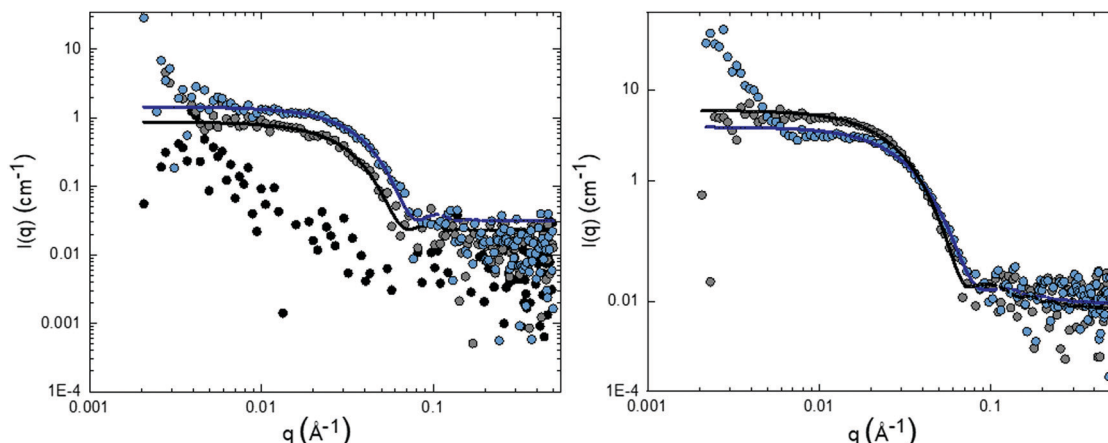


**Fig. 5** SANS data collected for mixtures of pNIPAM and triblock-copolymer surfactant. Circles represent raw data and lines the corresponding fits. The left is data collected at 25 °C, the right data collected at 40 °C. The black plot is pure d-pNIPAM (0.3 wt%), the grey plot is pure triblock-copolymer (0.75 wt%) and the blue plot is a mixture of d-pNIPAM (0.3 wt%) and triblock-copolymer (0.75 wt%). The error bars have been removed for clarity, the SANS data including error bars can be found in the ESI† (Fig. S7).

**Table 4** Summary of the SANS data collected for mixtures of d-pNIPAM (0.3 wt%) and triblock-copolymer surfactant (0.75 wt%). The model used to fit this data was the polymeric micelle model. Radius ( $r$ ), volume ( $V$ ), aggregation number ( $N_{\text{agg}}$ )

Sample	$r_{\text{core}}$ (Å)	$R_g$ (Å)	$V$ of core (Å $^3$ )	$V$ of corona (Å $^3$ )	$N_{\text{agg}}$	$N$ density (10 $^{15}$ cm $^3$ )
Triblock 25 °C	61.5	15.7	191 150	35 925	18	0.044
Triblock 40 °C	55.1	15.7	66 360	59 447	72	0.71
Mixture 25 °C	55.0	15.7	254 830	37 780	18	0.45
Mixture 40 °C	46.8	15.7	64 574	66 466	72	0.044

Evidence that the polymers associate can be found when looking at the absolute intensities of the triblock-copolymer micelle signal. At low temperatures, the absolute intensity for the mixture of triblock-copolymer and pNIPAM is higher than for the pure triblock-copolymer system. However, when looking at the absolute intensity for the high temperature mixture, there is a decrease compared to the pure triblock-copolymer system. This is evidence that at high temperatures the triblock-copolymer associates to the pNIPAM microgels. When analysing the absolute intensities it can be observed that approximately 37% of the triblock-copolymer has associated to the pNIPAM microgels. It is unclear for the mixed sample at elevated temperatures whether the signal is due to there being free micelles in solution, or micelles adsorbed to the pNIPAM microgel surface, as the signals would be indistinguishable. However it can still be concluded that some of the triblock-copolymer has associated to the pNIPAM, due to the decrease in absolute intensity of the micelle scattering signal.

In the high temperature mixtures there is also evidence of larger scattering objects (Fig. 5, right, blue data), not present in the low temperature mixed signal (Fig. 5, left, blue data). It can be assumed that the scattering from the larger object is due to triblock-copolymer being present in the object, as the d-pNIPAM was found to be contrast matched with the solvent. When analysing this low  $q$  data using a Guinier plot, the  $R_g$  of the object calculated was 55 nm (Fig. S9, ESI†). The radius of a collapsed d-pNIPAM microgel is approximately 25 nm and the diameter of the triblock-copolymer micelle is approximately

20 nm at 40 °C, both measured using dynamic light scattering. Therefore, this radius of gyration is consistent with a slightly swollen pNIPAM microgel decorated with triblock-copolymer surfactant micelles, rather than aggregates of pNIPAM microgels. This indicates that micelle bridging is the likely mechanism for gelation in this system observed at higher concentrations. Due to the limited data set, further details about the structure of the larger object cannot be obtained.

### 3.4 Effect of pNIPAM cross-link distribution

Further evidence that the association of these polymers at elevated temperature is responsible for the gelation, is that the degree of microgel cross-linking affects the ability of the system to gel. Particles were synthesised using a monomer feeding method to produce mono-disperse, uniformly cross-linked (UCL) pNIPAM microgels.<sup>46</sup> It was observed that UCL particles do not form gels in the presence of triblock-copolymer. This provides evidence for the need for the polymer to penetrate the particles in order for the gelation mechanism to be successful. pNIPAM microgels are known to have a core–shell structure, where the particles consist of a densely cross-linked core and a periphery of linear loosely cross-linked polymer. A particle with a UCL internal structure would be less accessible to penetration by the polymer. When investigating the penetration of PEO into pNIPAM-*co*-acrylic acid microgels, it was seen that the amount of PEO adsorbed decreased with increased cross-linking.<sup>43</sup> A UCL polymer would also be less stable to depletion, indicating again that depletion is not the mechanism for gelation in this system.

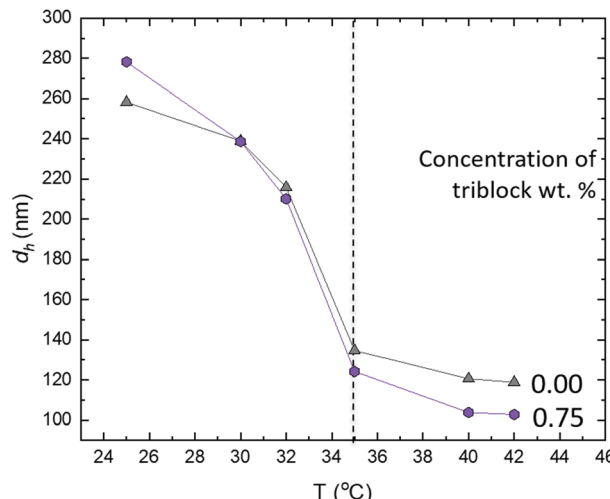


**Fig. 6** DLS data showing the behaviour of uniformly cross-linked particles in the presence of triblock-copolymer. Pure pNIPAM (black triangles), 0.3 wt% triblock-copolymer, 0.75 wt% pNIPAM (purple triangles). The dashed line indicates the temperature where an increase in hydrodynamic diameter is observed for conventionally synthesised pNIPAM.

It was observed using DLS that at temperatures above the  $T_{VPT}$  of pNIPAM there was no observable interaction between the UCL pNIPAM particles and triblock-copolymer. There is little evidence of the triblock-copolymer increasing the hydrodynamic diameter from DLS results, the effect observed for conventionally synthesised pNIPAM. This indicates that the interaction between these species is weaker or not present, likely due the triblock-copolymer being less able to penetrate the particles. This is summarised in Fig. 6. A comparison of the gels that result due to the interaction of triblock-copolymer with UCL and conventional pNIPAM are included in the ESI† (Fig. S11).

Further evidence for the triblock-copolymer not associating with the UCL particles can be observed when looking at the PDI of the samples (Fig. S6, ESI†). Like for the conventional pNIPAM particles, there is an increase in the PDI for the mixtures compared to pure pNIPAM samples. However, for UCL particles this increase is evident over the whole temperature range, whereas for conventional pNIPAM particles, there is a noticeable decrease in the PDI above the  $T_{VPT}$ . This shows again that there is no association of the triblock-copolymer to the UCL particles.

Charge screening was also suggested as an alternative mechanism for the reversible gelation, as pNIPAM microgels carry some residual charge, and the addition of electrolytes would lead to colloidal instability. This effect would be heightened at elevated temperature as the particles are no longer sterically stabilised due to the linear polymer particle periphery. Even though pNIPAM is a neutral polymer, it has been shown in the literature to carry charge due to the initiator used.<sup>54</sup> The triblock-copolymer used as part of this study is uncharged, and when comparing the conductivities of the minimum concentration of salt and triblock-copolymer required to make the particles gel, the difference is considerable. Another indicator that charge screening is not responsible for the gelation in this system is that salt is capable of gelling the UCL polymer particles

when polymeric triblock-copolymer is not, suggesting again that the mechanism is not a result of charge screening.

In a similar experiment, triblock-copolymer surfactant was added to a samples of preheated (collapsed) pNIPAM microgels. As seen for the UCL particles, preheated pNIPAM microgels do not form gels in the presence of triblock-copolymer surfactant, again highlighting how the periphery of the microgels is integral to gelation. The same sample was then cooled to room temperature and then heated above the  $T_{VPT}$  and formed gels as expected, showing that the concentration used is capable of forming gels when the periphery of the microgel particle is accessible. Images of the experiments conducted using these samples are included in the ESI† (Fig. S12).

### 3.5 Linear pNIPAM

The interaction between triblock-copolymer and linear pNIPAM was also investigated. When linear pNIPAM is heated above the lower critical solution temperature, the linear polymer becomes immiscible in water and precipitates, due to the increased hydrophobicity with temperature.<sup>55</sup> This was observed for the linear pNIPAM synthesised as part of this work. When comparing the stability of linear pNIPAM solutions with and without triblock-copolymer, significantly less precipitate forms in the presence of triblock-copolymer (Fig. 7, bottom left). The samples were imaged using differential interference contrast microscopy (DIC), the results of which are included in Fig. 7, to compare the macroscopic observations with microscopic images. The results show a featureless liquid at 25 °C for the pure linear pNIPAM (Fig. 7, top left). When the linear pNIPAM is heated above the lower critical solution temperature, the sample shows

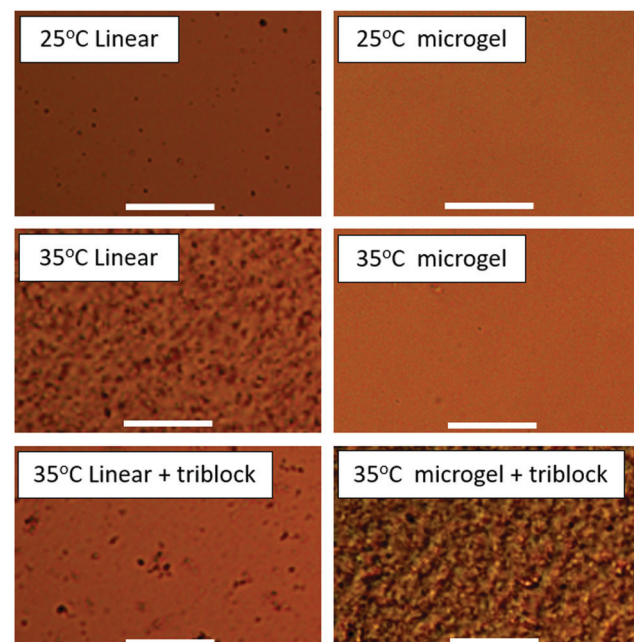


**Fig. 7** DIC images comparing linear pNIPAM (left column) and pNIPAM microgels (right column). Concentrations used for the images are 1 wt%, at 25 °C (top), at 35 °C (center), at 35 °C (bottom) with 6 wt% triblock-copolymer. Scale bar 80 μm.

the appearance of precipitated polymer (Fig. 7, middle left). For the sample with triblock-copolymer, again a featureless liquid is observed at 25 °C, however, at elevated temperatures, there is considerably less precipitate present and there is the appearance of isolated aggregates forming (Fig. 7, bottom left). These images show that the triblock-copolymer has associated with the pNIPAM at high temperatures, and as a result solubilises the pNIPAM and prevents precipitation. This further confirms that this association must be a vital part of the mechanism for the gelation of these species. The equivalent microgel samples are included to highlight the difference in behaviour of linear pNIPAM and pNIPAM microgels (Fig. 7, right).

The mechanism for association is the same as that predicted with microgels, where the triblock-copolymer can increasingly form hydrogen bonds with the amide group with elevated temperature as pNIPAM becomes increasingly hydrophobic. However, for linear pNIPAM this acts to stabilise the linear polymer which is not colloidally stable on heating, where the associated PEO chains remain soluble in water at temperatures above the  $T_{VPT}$ . When looking at high concentrations of mixtures of triblock-copolymer and linear pNIPAM there is evidence that this stabilization mechanism breaks down, as the aggregated polymer is observed using DIC microscopy at high temperatures. This effect could indicate the possibility that high concentration samples of linear polymer and triblock-copolymer behave like the microgel samples, where with increased triblock-copolymer there is an ability of the aggregates to bridge and form gel networks. However, the concentrations required increases due to the much smaller size of the pNIPAM entities involved.

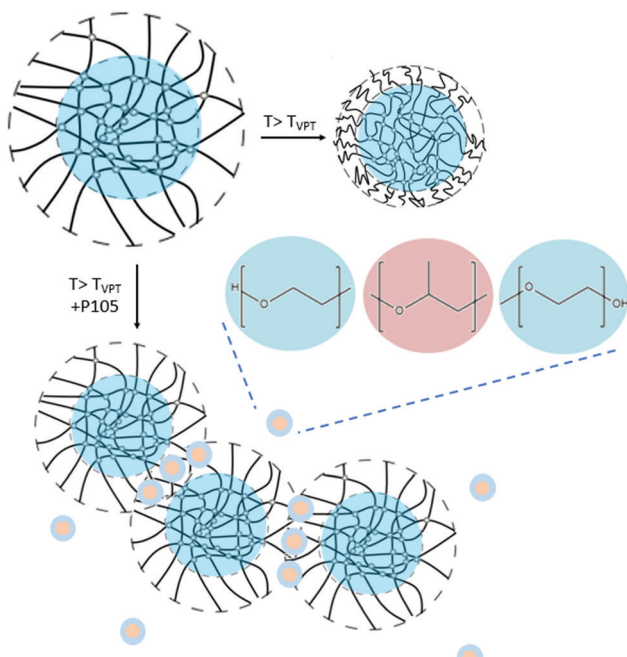


**Fig. 8** Mechanism for the gelation of triblock-copolymer surfactant and pNIPAM at elevated temperature. In this scheme the triblock-copolymer surfactants are assumed to bridge the particles while in the form of micelles. Scheme is not to scale.

### 3.6 Proposed associative mechanism

From the data provided in this manuscript, we believe the most likely mechanism for bridging is through triblock-copolymer micelles. PEO is known to penetrate pNIPAM microgels, however previously, it has not been suggested in the literature that this association is temperature responsive. We propose that the bridging occurs through the hydrogen bonding interaction of pNIPAM amine group and the ether groups on the PEO chain on heating. Confocal microscopy reveals that the polymer associate, SANS and DLS reveal that the size of the associated object is of order a pNIPAM microgel decorated with triblock-copolymer micelles. By altering the cross-link density we reveal that the surfactant must penetrate inside the microgel particles, as when the periphery of the particle is inaccessible gels are not observed. A schematic of the hypothesised association is included in Fig. 8.

## 4 Conclusions

In this work, we have demonstrated the temperature dependent association of a non-ionic polymeric surfactant and pNIPAM microgels, with the association providing a mechanism for the formation of percolating gel networks. We have demonstrated that these species only interact at temperatures above 35 °C, through DLS results showing that the diameter of the pNIPAM microgels is equivalent to that of pNIPAM alone until heated above their  $T_{VPT}$ , where a large increase is observed. The association of the species was confirmed using confocal microscopy, where both species were shown to be present in the gel network. This association is a gelation mechanism not seen before for pNIPAM microgels, where association of the polymers results in gelation. We also provide evidence that the mechanism is dependent on the cross-link distribution inside the particles, where only particles with a fuzzy corona can form gel networks through this mechanism, further providing evidence of this unique gelation mechanism. We believe this could provide further insight into the high concentration phase behaviour of these soft colloids. This system could be used as a model binary gel system, and aid the design of future systems. This material could also have applications for biomedical research, especially in the field of injectable tissue scaffolds.

## Conflicts of interest

There are no conflicts to declare.

## Acknowledgements

We gratefully acknowledge contributions by undergraduate project students Joe Stephens, Abigail Coveney and Jonny Keen. SF is supported by a studentship provided by the Bristol Centre for Functional Nanomaterials (EPSRC grant EP/L016648/1). KB was supported by EPSRC (grant EP/P50483X/1) and Bayer CropScience. WL was supported by the China Scholarships Council. CPR acknowledges support from EPSRC (grants GR/M32320/01)

and ERC (consolidator grant NANOPRS, project number 617266). JSvD thanks Professor Brian Vincent for many discussions on polymer colloids. We would like to thank Craig Davies, Croda, for supplying the Synperonic PE/P105. We would also like to acknowledge ISIS for the beam time (RB 1910080) and Sarah Rogers, the beam line scientist at SANS2D.

## Notes and references

- 1 J. A. Bonham, M. A. Faers and J. S. van Duijneveldt, *Soft Matter*, 2014, **10**, 9384–9398.
- 2 Y. Gao, X. Li and M. J. Serpe, *RSC Adv.*, 2015, **5**, 44074–44087.
- 3 H. Dalmont, O. Pinprayoon and B. R. Saunders, *Langmuir*, 2008, **24**, 2834–2840.
- 4 H. Senff and W. Richtering, *J. Chem. Phys.*, 1999, **111**, 1705–1711.
- 5 D. Klinger and K. Landfester, *Polymer*, 2012, **53**, 5209–5231.
- 6 B. Saunders, *Adv. Colloid Interface Sci.*, 1999, **80**, 1–25.
- 7 M. Yang, C. Liu, Y. Lian, K. Zhao, D. Zhu and J. Zhou, *Soft Matter*, 2017, **13**, 2663–2676.
- 8 K. N. Plunkett, X. Zhu, J. S. Moore and D. E. Leckband, *Langmuir*, 2006, **22**, 4259–4266.
- 9 I. Bischofberger, D. C. E. Calzolari, P. De Los Rios, I. Jelezarov and V. Trappe, *Sci. Rep.*, 2014, **4**, 1–7.
- 10 H. Du, R. Wickramasinghe and X. Qian, *J. Phys. Chem. B*, 2010, **114**, 16594–16604.
- 11 C. Wu and S. Zhou, *J. Polym. Sci., Part B: Polym. Phys.*, 1996, **34**, 1597–1604.
- 12 K. Kubota, *Polym. J.*, 1990, **22**, 1051–1057.
- 13 X. Sui, X. Feng, A. Di Luca, C. A. van Blitterswijk, L. Moroni, M. A. Hempenius and G. J. Vancso, *Polym. Chem.*, 2013, **4**, 337–342.
- 14 L. M. Lira, K. A. Martins and S. I. C. d. Torresi, *Eur. Polym. J.*, 2009, **45**, 1232–1238.
- 15 A. Gandhi, A. Paul, S. O. Sen and K. K. Sen, *Asian J. Pharm. Sci.*, 2015, **10**, 99–107.
- 16 H. Masoud and A. Alexeev, *ACS Nano*, 2012, **6**, 212–219.
- 17 L. Klouda and A. G. Mikos, *Eur. J. Pharm. Biopharm.*, 2008, **68**, 34–45.
- 18 A. Scotti, M. C. Rheinstädter, M. Bleuel, T. Hoare, E. Mueller, W. Richtering and R. J. Alsop, *Langmuir*, 2017, **34**, 1601–1612.
- 19 M. Stieger, W. Richtering, J. S. Pedersen and P. Lindner, *J. Chem. Phys.*, 2004, **120**, 6197–6206.
- 20 F. Scheffold, P. Diaz-Leyva, M. Reufer, N. Ben Braham, I. Lynch and J. L. Harden, *Phys. Rev. Lett.*, 2010, **104**, 2–5.
- 21 J. N. Immink, J. J. E. Maris, J. J. Crassous, J. Stenhammar and P. Schurtenberger, *ACS Nano*, 2019, 3292–3300.
- 22 R. H. Pelton and P. Chibante, *Colloids Surf.*, 1986, **20**, 247–256.
- 23 J. Gao and B. J. Friskin, *Langmuir*, 2003, **19**, 5217–5222.
- 24 K. S. Oh, J. S. Oh, H. S. Choi and Y. C. Bae, *Macromolecules*, 1998, **31**, 7328–7335.
- 25 E. Zaccarelli, *J. Phys.: Condens. Matter*, 2007, **19**, 32.
- 26 P. O. Kinell, *Nature*, 2008, **164**, 43–44.
- 27 C. P. Royall, S. R. Williams, T. Ohtsuka and H. Tanaka, *Nat. Mater.*, 2008, **7**, 556–561.
- 28 K. Pickrahn, B. Rajaram and A. Mohraz, *Langmuir*, 2010, **26**, 2392–2400.
- 29 Y. Otsubo, *Langmuir*, 1990, **6**, 114–118.
- 30 R. Fantoni, A. Giacometti and A. Santos, *J. Chem. Phys.*, 2015, **142**, 224905.
- 31 C. Zhao, G. Yuan and C. C. Han, *Soft Matter*, 2012, 7036–7043.
- 32 K. Bayliss, J. S. Van Duijneveldt, M. A. Faers and A. W. Vermeer, *Soft Matter*, 2011, **7**, 10345–10352.
- 33 D. Paloli, P. S. Mohanty, J. J. Crassous, E. Zaccarelli and P. Schurtenberger, *Soft Matter*, 2013, **9**, 3000–3004.
- 34 A. M. Alsayed, *Science*, 2005, **309**, 1207–1210.
- 35 J. Mattsson, H. M. Wyss, A. Fernandez-Nieves, K. Miyazaki, Z. Hu, D. R. Reichman and D. A. Weitz, *Nature*, 2009, **462**, 83–86.
- 36 L. A. Lyon and A. Fernandez-Nieves, *Annu. Rev. Phys. Chem.*, 2012, **63**, 25–43.
- 37 P. Soares, M. Godinho, S. Fernandes, C. Echeverria and J. Borges, *Gels*, 2018, **4**, 54.
- 38 J. M. van Doorn, J. Sprakler and T. E. Kodger, *Gels*, 2017, **3**, 21.
- 39 T. Gan, Y. Zhang and Y. Guan, *Biomacromolecules*, 2009, **10**, 1410–1415.
- 40 I. Bischofberger and V. Trappe, *Sci. Rep.*, 2015, **5**, 15520.
- 41 D. Cheng, Y. Wu, Y. Guan and Y. Zhang, *Polymer*, 2012, **53**, 5124–5131.
- 42 M. Bradley, J. Ramos and B. Vincent, *Langmuir*, 2005, **21**, 1209–1215.
- 43 M. Bradley and B. Vincent, *Langmuir*, 2005, **21**, 8630–8634.
- 44 W. McPhee, K. C. Tam and R. Pelton, *J. Colloid Interface Sci.*, 1993, **156**, 24–30.
- 45 J.-M. Meijer, PhD thesis, University of Utrecht, 2015.
- 46 R. Acciaro, T. Gilanyi and I. Varga, *Langmuir*, 2011, **27**, 7917–7925.
- 47 J. Gao and B. J. Friskin, *Langmuir*, 2003, **19**, 5212–5216.
- 48 P. Alexandridis, J. F. Holzwarth and T. A. Hatton, *Macromolecules*, 1994, **27**, 2414–2425.
- 49 G. J. Swanson, *Water Well J.*, 1998, **52**, 34.
- 50 J. S. Pedersen and M. C. Gerstenberg, *Macromolecules*, 1996, **29**, 1363–1365.
- 51 S. Sbeih, P. S. Mohanty, M. R. Morrow and A. Yethiraj, *J. Colloid Interface Sci.*, 2019, **552**, 781–793.
- 52 K. Mortensen, *Polym. Adv. Technol.*, 2001, **12**, 2–22.
- 53 K. Mortensen, *J. Phys.: Condens. Matter*, 1996, **8**, A103–A124.
- 54 Y. Utashiro, M. Takiguchi and M. Satoh, *Colloid Polym. Sci.*, 2017, **295**, 45–52.
- 55 H. G. Schild, *Prog. Polym. Sci.*, 1992, **17**, 163–249.